



# A Compact Multi-Frequency Circular Patch Antenna Embedded with Metamaterial Resonators

Asit K. Panda

**Abstract:** In this paper, a novel method to achieve tri-band performance for both reduced and conventional size circular microstrip patch antenna (CPA) loaded with low loss metamaterial unit cell is presented. The proposed tri-band CPA is based on metamaterial structure called complementary skewed omega type resonator (CSOR). The conventional CPA operating with 5.1GHz loaded with a pair of symmetric CSORs on the ground plane excites three working frequencies. Beside miniaturization, this work mainly focuses on multiband operation with performance enhancement of the circular patch antenna. Numerical simulation of the proposed antenna appears that the operating frequencies of each band can tune separately. Good matching and stable radiation pattern with a satisfactory gain is achieved in the working frequency band. A good concord between simulation and measurement results validate the design method.

**Keywords:** Metamaterial, complementary skewed omega resonator (CSOR), circular patch antenna (CPA), tri-band.

## I. INTRODUCTION

With the speedy advancement of wireless and RF system, the interest for designing smaller size and multi-frequency antennas is attractive for wireless terminals. The challenges are to have a small size, miniaturization, and incorporation with PCB [1].

Recently, engineered materials such as metamaterial (MTMs) offer an intangible direction for realizing miniaturized antennas with excellent performance which likewise provide a reasonable route to double or multi-mode operations reported in [2-3]. It mainly focuses on miniaturization, better radiation performance.

Electrically small resonant rectangular patch antennas using complementary SRRs (CSRRs) & split ring resonator (SRRs) MTM unit cells have received much attention in the design dual and multiband small antennas in the microwave regime.

Dual-band small resonating antennas were investigated [4-7] by loading a pair of or multi CSRR unit cells either on the ground plane or radiating surface.

But by etching CSRR unit cells in the ground plane or from radiator surface, the gain and efficiency of such antennas degrade considerably because of the introducing of loss by the CSRR at the operating frequency simulated by the MTM CSRR unit cell. Later, it was concluded that most of these MPA embedded with small size MTM unit cells act as a resonator, but in practice, it is hardly used as a good antenna.

However, it has been seen that the radiation performances such as gain and directivity of these miniaturized resonating antennas decrease acutely because of the decrease of size.

To increase the gain of the MPA, Xie *et al* and his group realized numerically and experimentally a new dual-frequency antenna by etching two and more CSRRs in the ground plane of the MPA. [8]. Later, several small antennas are successfully demonstrated in the literature that provides dual-band performances with enhanced directivity gain performance by using two or more complementary split-ring resonator. Be that as it may, such antennas need a huge area for realization [9-10].

Even as the vast majority of the proposed approaches cited in the research articles demonstrate a single or dual operating band for a metamaterial-based small antenna. This negates to the development of next-generation wireless communication systems, of which multi-frequency applications have turned out to be crucial. Multi-mode antennas incorporating with CSRR have been proposed [11-13].

In this paper, a low profile multi-frequency CPA embedded with two low loss complementary skewed omega resonator (CSOR) MTM unit cells on the ground plane has been investigated. Beside miniaturization, this proposed work mainly focuses on multiband operation with performance enhancement of the circular patch antenna.

## II. ANTENNA CONFIGURATION.

The configuration of a multiband CPA loaded with metamaterial resonators has been depicted in Fig. 1. It is based on circular patch loaded with two symmetrical complementary skewed omega resonators (CSORs) MTM unit cell. This would excite the circular patch as being placed on a double positive material and single negative material (DPS-SNG) medium and feed at the positive side.

Manuscript received on February 10, 2020.

Revised Manuscript received on February 20, 2020.

Manuscript published on March 30, 2020.

\* Correspondence Author

Asit Kumar Panda\*, ECE dept. National Institute of Science & Technology (NIST), Palur Hills, Golanthara, Berhampur, Odisha, India.  
Email: [asitkp.nist@gmail.com](mailto:asitkp.nist@gmail.com)

© The Authors. Published by Blue Eyes Intelligence Engineering and Sciences Publication (BEIESP). This is an open access article under the CC BY-NC-ND license (<http://creativecommons.org/licenses/by-nc-nd/4.0/>)

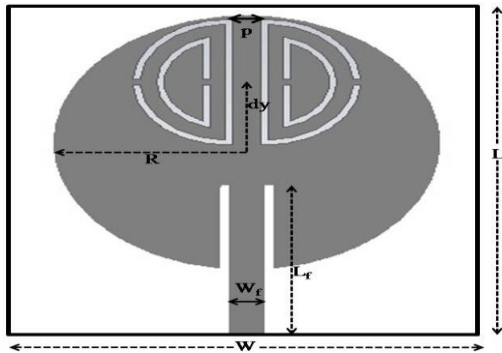


**Fig. 1 Configuration of the tri-band antenna embedded with dual CTORs.**

The CSORs are introduced in the ground plane along the radiating edges and at a distance of ‘*dx*’ away from the centre of the transmission feed line. A series of parametric training was executed numerically using simulation to find the best position of CSORs in *x*- and *y*-directions from the centre, at which better impedance matching, radiation efficiency and gain in all the desired bands can be achieved.

The metamaterial loaded multiband CPA was designed using a low loss FR4 epoxy microwave laminator with substrate thickness (*h*) is 1.6 mm, and dielectric constant ( $\epsilon_r$ ) is 4.4, loss tangent factor equal to 0.02.

The design process starts with a basic circular patch operating at 5.1 GHz  $TM_{01}$  fundamental frequency mode. The geometrical parameter of the CPA is determined from the following equations [14].

$$a = \frac{F}{\left(1 + \frac{2h}{\pi\epsilon_r F} \left[ \ln\left(\frac{\pi F}{2h}\right) + 1.7726 \right] \right)^{0.5}} \quad (1)$$

Where

$$F = \frac{8.7911 \times 10^9}{f_r \sqrt{\epsilon_r}} \quad (2)$$

Where

*f<sub>r</sub>* is the resonating frequency, ‘*h*’ is substrate thickness in mm. The final optimized parameters used in the design of the multi-mode CPA are depicted in Table I.

**Table – I: Dimensions of the Multi-band CPA.**

Parameter	R	dy	P	W	L	W <sub>f</sub>	L <sub>f</sub>
Dimension (mm)	21	4.6	2	27	30	1.92	13

### III. MTM UNIT CELL DESIGN METHODOLOGY AND EM CHARACTERIZATION

In this section, the electromagnetic characteristics and electric resonance frequency behaviour of a low loss complementary skewed omega resonator (CSOR) MTM unit cell structure is discussed. Compared with conventional CSRR structure reported the literature, the CSOR metamaterial unit cell provides a better method of miniaturization with slight loss and dual-band negative permittivity characteristics in microwave frequency regime [15]. It is also found that the skewed omega dual-band resonator structure is further compacted compared to the existing electric resonators utilized to attain negative permittivity property in dual-band. To determine its resonant

characteristics and retrieve the constitutive parameter (effective permittivity) of the metamaterial unit cell through EM simulation, a wave-guide set up with infinite periodic boundary condition is used. Fig. 2 shows the geometrical configuration of CSOR.

**Table- II: CSOR MTM unit cell dimension.**

Parameter	a	c	d	g	ax	ay
Dimension (mm)	3.8	0.4	0.9	0.5	8.8	6.1

It provides negative permittivity characteristics at the desired frequency when excited with the tangential electric field. In Table II, the geometrical dimensions of the CSOR are recorded.

The simulation has been made for a CSOR MTM unit cell using a perfect electric conductor (PEC) and perfect magnetic conductor (PMC) boundary conditions. The PEC and PMC boundary condition were assigned along X and Y-axes, respectively. The medium perpendicular to the Z-axis is modelled as the input/output ports. Then, the CSOR is excited by an EM wave propagating along the Z-axis (Fig.2). The approximate resonance frequency of CSOR can be calculated by using [16]. In Fig. 3 (a), the simulated S-parameter of the CSOR unit cell is presented. The spectral position of the resonating frequencies can be evaluated from the spectral location of the transmission minimum. It has been found that there are two pass-bands with reflection dips occurring at 3.86 and 6.8GHz respectively, where the electric resonances occurred nearby. The transmission peaks are nearly 0 dB and -1.01 dB level in the 1<sup>st</sup> and 2<sup>nd</sup> band respectively, and the spectral reflection power is around -20 dB at the peak resonating frequency of the first band while it is better than -50 dB in the second band.

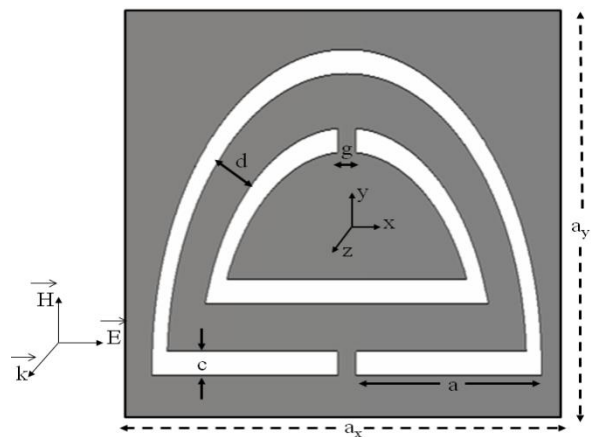


**Fig. 2 Geometrical configuration of CSOR MTM unit cell.**

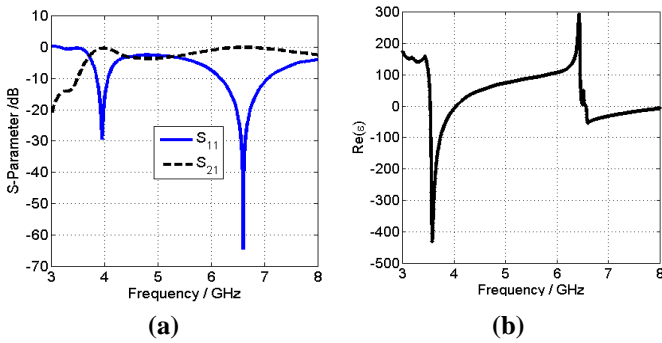


**Fig. 3: (a) S-Parameters of CSOR MTM resonator, (b) effective permittivity of CSOR.**

The effective retrieval properties of the designed complementary skewed omega resonator unit cell haven computed using the simulated Scattering factors obtained from numerical analysis, using the standard parameter retrieval method [17].

It is found that from 3.57 to 4.07 GHz and from 6.6 to 8.0GHz, the CSOR medium give negative permittivity (near the electric resonance of CSOR MTM unit cell) and the unit cell behaves as SNG medium in these dual operating frequency range (Fig. 3(b)). The figure of merit (FOM) of the designed CSOR unit cell has been depicted in Fig.4 for the desired single negative band and it varies from 0.93 to 0.012 in 1<sup>st</sup> SNG band (3.57-4.07 GHz) and from 0.45 to 0.02 for the 2<sup>nd</sup> SNG band (6.6-8.0GHz). A low value of the figure of merit (FOM) indicates a low loss inside the negative permittivity frequency bands [15].

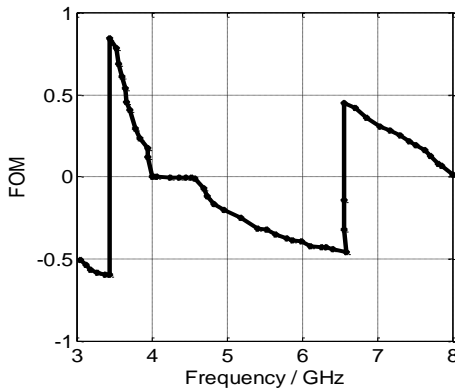


**Fig. 4: Figure of Merit (FOM) of CSOR MTM unit cell.**

**IV. RESULT & DISCUSSION**

The photography of the designed antenna model was shown in Fig.5. The fabricated was measured and compared with simulated results to verify its validity.

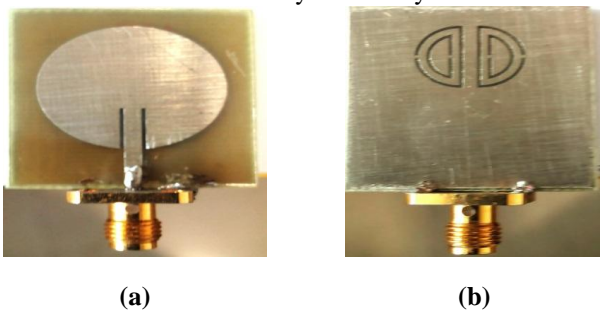


**Fig. 5: Prototype of the proposed antenna. (a) Front,(b) Back**

The comparison between simulated reflection coefficients of the CPA loaded with and without CSOR is illustrated in Fig.6.

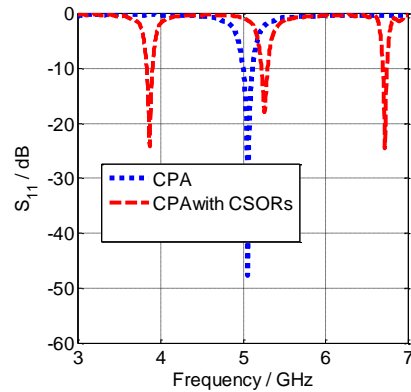


**Fig. 6: Simulated return loss of CPA embedded without and with CSOR resonators.**

From the results, it is clearly found that the conventional antenna resonated at 5.1GHz effectively with minimum reflection coefficient is less than -45dB at the peak resonating frequency. Fig.7 shows the co-plane and cross-plane of the simple CPA without CSOR. For the simple CPA, the measured gain was found to be nearly equal to 6.2dBi.

To generate tri-band, the conventional CPA was loaded with a pair of CSOR resonators. Assessments between numerical simulation & measured S11 of both the antennas have been depicted in Fig.8, which are in good agreement. By loading the CSOR resonators in the finite ground structure, multi-frequency resonate appeared at 3.86Gz, 5.25GHz and 6.72GHz respectively. The measured -10 dB impedance bandwidths are about 90 MHz for the 3.86 GHz (from 3.81 to 3.92 GHz); 100 MHz for the 5.25GHz (from 5.20 to 3.30 GHz); and 80 MHz for the 6.72 GHz (from 6.67 to 6.75 GHz).

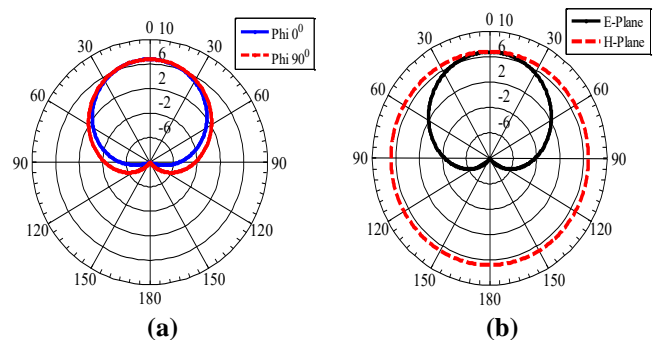


**Fig. 7: Numerical 2D directivity-gain radiation pattern of the conventional CPA at 5.1GHz. (a) co-plane for  $\Phi=0^\circ$ , (b) cross-plane for  $\Phi=90^\circ$ .**

In the designed tri-band antenna, the top layer circular radiating patch excites the 2<sup>nd</sup> resonant frequency at 5.1 GHz, whose resonance frequency can be determined from equation (1). From the simulated result of the proposed antenna (Fig.6), it is evident that by loading of the CSORs to the patch slightly shifted the fundamental resonant frequency of the circular radiating patch (2<sup>nd</sup> resonating frequency) from 5.1 GHz to 5.25GHz. These shifts of the resonating frequency to a higher value have been because of the existence of CSOR MTM resonator particles.

Since the fringing field behaviour of the radiating element changed followed by antennas electrical length reduced and hence the operating resonating band shifted to a little higher frequency. Hence, it suggests a reduction in the radiating patch dimension.

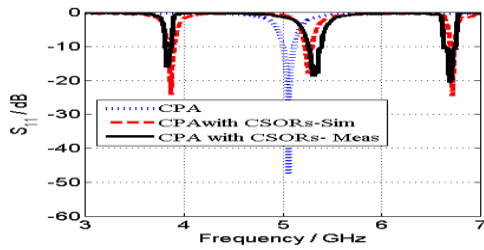


Fig. 8: Measured & Simulated magnitude of  $S_{11}$  of CPA without and with CSORs loading.

In contrast, CSORs are liable for 1<sup>st</sup> and 3<sup>rd</sup> frequency. The retrieval EM characteristics of the CSOR are accustomed to generate the 1st and 3<sup>rd</sup> resonance frequencies at 3.86GHz and 6.72GHz, respectively. The measured results demonstrated our proposed tri-band antenna design in that CSORs control each of the bands.

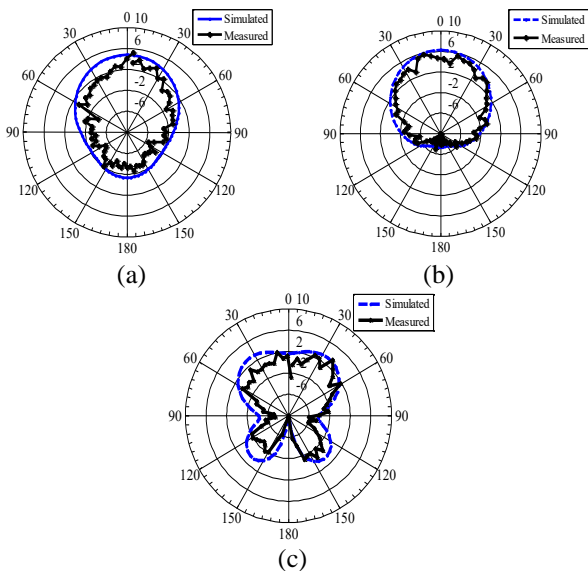


Fig. 9: Radiation patterns for  $\phi=0^\circ$  at (a) 3.86 GHz, (b) 5.25GHz and (c) 6.7 GHz.

The 2-D directivity radiation patterns at different frequency bands are measured at NIST FIST Lab. 2-D radiation patterns of CPA loaded with and without CSORs in the ground plane in both co- & cross –planes were-plane at 3.86, 5.25 and 6.72 GHz bands are revealed in Fig. 9 [a-c] respectively. A decent agreement between simulated and measurement of directivity pattern results were found. As shown both the results provide nearly omnidirectional radiation pattern in XZ-plane and bi-directional radiation pattern in XY-plane.

The measured peak gain of the proposed antenna in the broadside direction against the frequency is depicted in Fig. 10. The maximum peak gain about 4.7dBi in 3.86 GHz band (3.81- 3.92 GHz), 6.4dBi in the 5.25 GHz band (5.20-5.30 GHz) and 4.25dBi in the 6.72 GHz (6.67-6.75 GHz) was found in measurement.

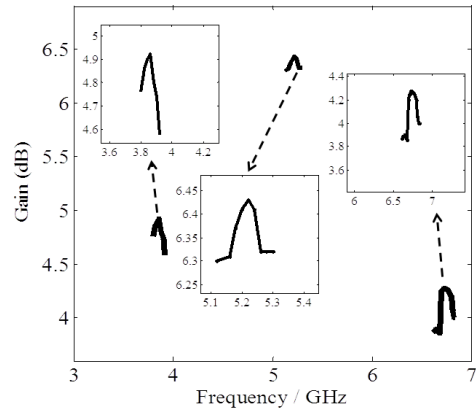


Fig. 10: Measured gain curve.

To enable a clear understanding of the working operating bands, the E-field distribution of the conventional CPA and the proposed CPA loaded with CSORs at the desired operating frequencies are depicted in Fig. 11 and Fig. 12 respectively.

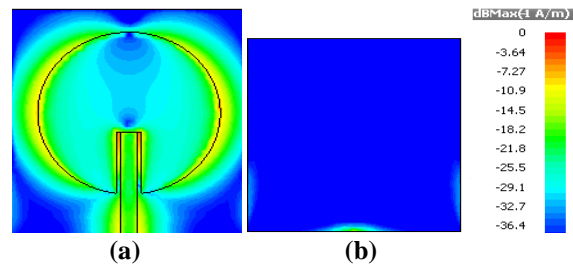
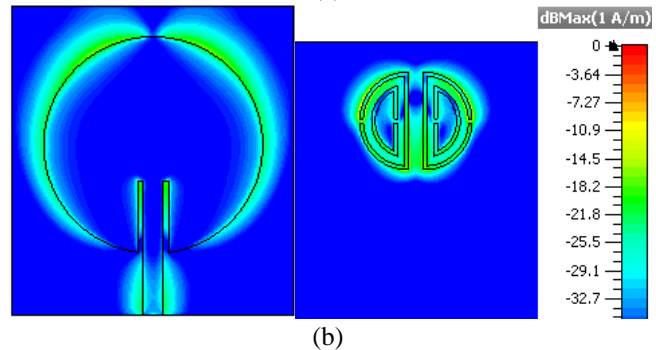
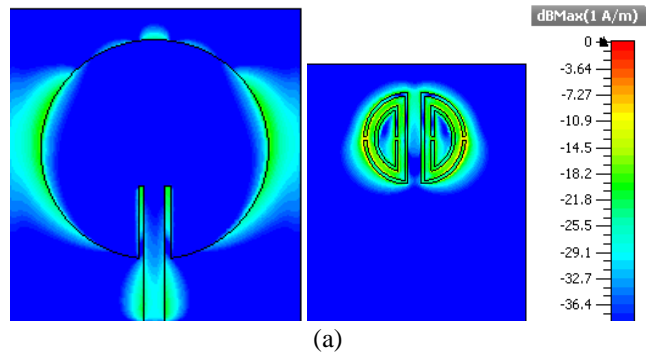
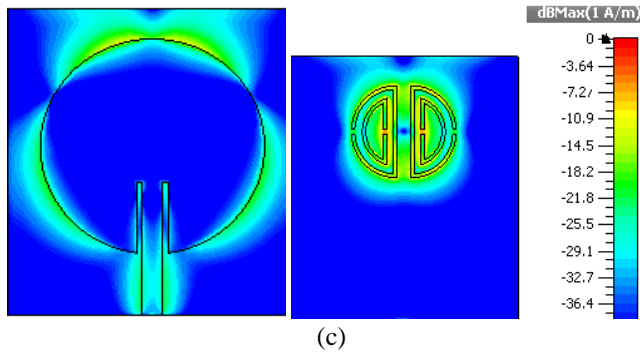


Fig. 11: The simulated current distribution of the CPA at 5.1GHz: (a) on patch and (b) on grounds.





**Fig. 12: The simulated current distributions of the CSORs loaded CPA on patch (left) and the ground (right) at: (a) 3.86 GHz, (b) 5.25 GHz and (c) 6.7GHz.**

The performance (in terms of the frequency band, size) of the proposed design and other metamaterial loaded planar antenna and other referred antenna models published recently are compared to table III. It is found that the proposed multiband antenna model provides better miniaturization and multi-mode applications are the main operational advantage of the proposed design. The low profile of the suggested tri-band antenna system will be suitable for the size of most RF & modern mobile computing components.

**Table- III: Comparison between the proposed MTM loaded Antennas work others**

Ref.	Frequency bands (GHz)	Gain in dBi	Antenna Size (mm <sup>2</sup> )
[9]	2.4, 5.8	5.17 at 2.4 7.12 at 5.8	182.52
[10]	3.1, 4.7	5.9 at 3.1 6.26 at 4.7	70×70
[1]	2.4, 3.4, 5.2	-1, 1, 4	30×34
[7]	3.83, 5.45	4.7, 6.2	17.7×17.5
[8]	3.71, 5.28	5.2, 6.4	17.7×17.5
This work	3.86, 5.25, 6.72	4.7, 6.4, 4.25	27×30

## V. CONCLUSIONS

A novel miniaturised tri-band metamaterial inspired CPA was presented in this paper. The proposed tri-band CPA was based on metamaterial structure called complementary skewed omega type resonator (CSOR). The conventional CPA operating with 5.1GHz loaded with a pair of symmetric CSORs on the ground plane excites three working frequencies. The suggested antenna operates at 3.86GHz, 5.25 GHz and 6.72 GHz respectively with a compact size of 27×30×1.6 mm<sup>3</sup>. Numerical simulation of the designed antenna shows that each of the frequency bands can be tuned separately. A better matching, omnidirectional radiation property with steady gain over each working bands was realized. Good conformity between measurement and simulations outcomes approves the design approach.

## REFERENCES

1. S.C. Basaran, and Y.E. Erdemli, "A dual band split-ring monopole antenna for WLAN applications," *Microw. Opt. Technol. Lett.*, vol. 51, 2009, pp. 2685–2688.

2. Xu H.-X., Wang G.-M. and M.-Q. Qi, "A miniaturized triple-band metamaterial antenna with radiation pattern selectivity and polarization diversity," *Progress In Electromagnetics Research*, vol. 137, 2013, pp. 275-292.
3. H. X. Xu et al., "Analysis and Design of Two-Dimensional Resonant-Type Composite Right/Left-Handed Transmission Lines With Compact Gain-Enhanced Resonant Antennas," *IEEE Transactions on Antennas and Propagation*, vol. 61, 2013, pp. 735-747.
4. J. Malik and M. V. Kartikeyan, "Metamaterial inspired patch antenna with l-shape slot loaded ground plane for dual band (WiMAX/WLAN) applications," *Progress in Electromagnetics Research Letters*, vol. 31, 2012, pp. 35-43.
5. N. Ortiz, F. Falcone, and M. Sorolla, "Dual band patch antenna based on complementary rectangular split ring resonators," *2009 Proceeding of Asia-Pacific Microwave Conference (APMC)*, pp. 2762-2765, 2009.
6. H. Zhang, Y.-Q. Li, X. Chen, Y.-Q. Fu, and N.-C. Yuan, "Design of circular/dual-frequency linear polarization antennas based on the anisotropic complementary split ring resonator," *IEEE Trans. Antennas Propagat.*, vol. 57, 2009, pp. 3352-3355.
7. Y. H. Xie, C. Zhu, L. Li, and C. H. Liang, "A novel dual-band metamaterial antenna based on complementary split ring resonators," *Microwave Opt. Technol. Lett.*, vol. 54, 2012, pp. 1007–1009.
8. Y. Xie, L. Li, C. Zhu, and C.-H. Liang, "A novel dual-band patch antenna with complementary split ring resonators embedded in the ground plane," *Progress In Electromagnetics Research Letters*, vol. 25, 2011, pp. 117-126.
9. I. Sassi, L. Talbi, and K. Hettak, "A novel dual-band antenna based on corrugated slotted-complementary split-ring resonators," *Microw. Opt. Technol. Lett.*, vol. 57, 2015, pp. 2310–2315.
10. K. Kandasamy, B. Majumder, J. Mukherjee and K. P. Ray, "Dual-Band Circularly Polarized Split Ring Resonators Loaded Square Slot Antenna," *IEEE Transactions on Antennas and Propagation*, vol. 64, 2016, pp. 3640-3645.
11. Y. Dong, H. Toyao and T. Itoh, "Design and Characterization of Miniaturized Patch Antennas Loaded with Complementary Split-Ring Resonators," *IEEE Transactions on Antennas and Propagation*, vol. 60, 2012, pp. 772-785.
12. S. C. Basaran, U. Olgun and K. Sertel, "Multiband monopole antenna with complementary split-ring resonators for WLAN and WiMAX applications," *Electronics Letters*, vol. 49, 2013, pp. 636-638.
13. W. Ali, E. Hamad, M. Bassiuny, M. Hamdallah, "Complementary Split Ring Resonator Based Triple Band Microstrip Antenna for WLAN/WiMAX applications," *Radio engineering*, vol. 26, 2017, pp. 78-84.
14. A. Constantine Balanis, *Antenna Theory, Analysis and Design*, NY : John Wiley & Sons, Inc, 3rd Edition, 2005.
15. Asit K. Panda, Rabindra K. Mishra, Sudhakar Sahu, "A skewed omega for LHM characteristics," *Microw. Opt. Technol. Lett.*, vol. 58, 2016, pp. 847-850.
16. Asit K. Panda, Sudhakar Sahu and Rabindra K. Mishra, "Optimization of skewed omega for left-handed material characteristics," *J. Nanophoton.*, vol. 9, 2015, pp. 093039.
17. DR Smith, DC Vier, Th. Koschny, C.M. Soukoulis, "Electromagnetic parameter retrieval from inhomogeneous metamaterials," *Phys Rev E*, vol. 71, 2005, pp. 36617.

## AUTHORS PROFILE



**Dr. Asit Kumar Panda** is presently working as an Associate Professor, National Institute of Science & Technology (NIST), Berhampur, India. He received his Ph.D. degree in electronics engineering from KIIT University, Bhubaneswar and has done his M. Tech degree in ECE from BPUT, Odisha. He has researched extensively in the areas of Cognitive Commination, MIMO antenna and applications of metamaterial techniques. He has published over 20 learned papers in journals of repute, proceedings of conferences, seminars, and so forth. He is a member of IEEE Microwave & AP Society, life member IETE.